Comparative theoretical study of H_2Se adsorption and dissociation on ZnO($10\bar{1}0$), TiO_2(110), and Zn_2TiO_4(010)

Shiqiang Hao*
Department of Chemical Engineering, Carnegie Mellon University, Pittsburgh, Pennsylvania 15213, USA
(Received 20 May 2010; revised manuscript received 10 August 2010; published 9 September 2010)

Removal of corrosive or toxic species such as As, Se, and S is critical to the successful implementation of high efficiency integrated gasification combined cycle processes to utilize coal as a more environmentally friendly fuel. In this work we comparatively study the mechanisms of surface reaction of H_2Se on a regenerable sorbent, zinc orthotitanate (Zn_2TiO_4), and two constituent materials, ZnO and TiO_2, using first-principles density-functional theory. H_2Se adsorbs more strongly on the ZnO($10\bar{1}0$) and Zn_2TiO_4(010) surfaces than on the TiO_2(110) surface. Investigation of the dissociation rates shows that dehydrogenation should be facile on both Zn_2TiO_4 and ZnO while it is much slower on TiO_2. Evaluation of sublimation energies of Zn_2TiO_4 and ZnO suggests that Zn_2TiO_4 has higher thermal stability than ZnO due to addition of TiO_2, in agreement with experimental results.

DOI: 10.1103/PhysRevB.82.115414 PACS number(s): 68.43.Bc, 82.37.Np, 82.45.Jn

I. INTRODUCTION

The integrated gasification combined cycle is becoming a preferred way of providing the basis for turning coal into a fuel due to its high efficiency and minimal environmental impact. Cleaning coal fuel gas is a crucial step in this process. Although the hot gas desulfurization process has received extensive attention, removal of other corrosive or toxic species such as As, Se are also of great interest. It is thought that during coal gasification arsenic and selenium may form volatile toxic compounds that remain in the gas phase at high temperature, and may be released into the environment.[1,2] Currently, to clean up different contaminants, multiple sorbents with different operating conditions are required, which undoubtedly increases the complexity and cost of the process.[3] For example, the retention of H_2S(g) in the gasification process can be attained by using various Ca-based sorbents such as limestone and dolomite,[4] and the capture of species containing Na, K, Pb, and Cd can be carried out by using kaolin materials (mixture of SiO_2 and Al_2O_3).[5] Even though these materials are widely available, and stable at high temperatures, they normally generate a huge amount of solid residues and thus are not regenerable.

An alternative cost-effective strategy for removing all contaminants from the fuel gas would have a single unit operation and also allow sorbent regeneration to recover the contaminants in concentrated streams. It was found that zinc ferrites ($ZnFe_2O_4$) and zinc titanates (Zn_2TiO_4) have relatively high sulfur adsorption capacity with better high-temperature thermal stability than copper oxides.[6] However, the major disadvantage of zinc ferrites is their tendency to form high concentration of iron sulfate residuals and to undergo reductive degradation to FeO and Fe when exposed to highly reductive fuel gas environments. Compared to zinc ferrites, the use of zinc titanates improves regenerability and thermal stability.[6–8] At typical experimental condition, 550 °C, 1 bar and 2000 ppm H_2S, the reaction mechanism of zinc titanates with sulfur species is believed to be[9] $Zn_2TiO_4+2H_2S \rightarrow 2ZnS+TiO_2+2H_2O$ and regenerated by $ZnS+\frac{3}{2}O_2 \rightarrow ZnO+SO_2$ and $ZnO+TiO_2 \rightarrow Zn_2TiO_4$.

Even though zinc titanates are good candidates for retention of sulfur, the reaction mechanisms of multiple containments (H_2S, H_2Se, AsH_3, NH_3, and Hg, etc.) are not clear. Thus developing novel sorbent materials that are better suited to cleaning multiple contaminants with an acceptable energy cost is still a long term goal. In this paper, we focus on an examination of adsorption mechanisms and energetics on zinc orthotitanate Zn_2TiO_4 and two constituent materials ZnO and TiO_2. It would be not only interesting to understand the difference between them but also helpful in designing new materials. To this end, using first-principles methods, the initial surface reaction mechanisms of the uptake of Se by Zn_2TiO_4 and pure ZnO together with TiO_2 additive are studied.

II. CALCULATION METHOD

We used density-functional theory (DFT), within the generalized-gradient approximation with the Perdew-Wang 91 functional,[10] periodic boundary conditions and plane wave basis set as implemented in the Vienna *ab initio* simulation package[11] to obtain the relaxed geometries, as well as the total energies. The all-electron projector augmented wave potentials[12,13] have been used for all species. The cut-off energy for the plane-wave basis is 460 eV. The surface calculations reported here are based on relative stable slabs of 5-layer wurtzite ZnO($10\bar{1}0$),[14] 7-layer rutile TiO_2(110),[15] and 6-layer inverse spinel Zn_2TiO_4(010) (Ref. 16) each with 12 Å vacuum. Surface-energy calculations show that Monkhorst $2\times2\times1$, $3\times4\times1$, and $3\times3\times1$ k-point sampling in the Brillouin zone are sufficient for 60 atom cell ZnO($10\bar{1}0$), 54 atom cell TiO_2(110), and 56 atom cell Zn_2TiO_4(010) surfaces, respectively. This is reasonable since the denser k-point settings $3\times3\times1$, $4\times5\times1$ and $4\times4\times1$ only create 0.0026, 0.0001, and 0.0003 J/m^2 surface energy difference. Here, the surface energy is calculated by $\sigma=(E_{slab}-E_{bulk})/2A$, where E_{slab} is the total energy of slab, E_{bulk} is the bulk total energy of same number of slab atoms and A is the surface area. For the adsorption calculations, all

atomic positions but bottom layer atoms are relaxed until the forces exerted on them are less than 0.03 eV/Å. In our calculations, the bottom layer of each slab is not passivated by extra atoms, because charge neutral Zn-O and OTi_2O_2O trilayer units, respectively, induce zero dipole moment in the normal direction of wurtzite ZnO($10\bar{1}0$) and TiO_2(110), resulting in nonpolar characteristic. For Zn_2TiO_4(010), due to the complexity of the inverse spinel structure, we simply use clean surface without passivization. To identify the dissociation minimum energy paths, the climbing nudged elastic band (NEB) method[17] was used to investigate the dissociation barriers for adsorbates on all surfaces.

III. RESULTS

Before surface calculations, bulk properties of ZnO and TiO_2 are first investigated. To obtain correct bulk structure properties, a full lattice optimization is applied, which includes not only internal atomic positions but also stress tensor and cell volume. Compared with observed lattice constants of ZnO $a=3.2495$, $c=5.2069$ Å,[18] and TiO_2 $a=4.5937$, $c=2.9618$ Å,[18] the calculated results $a=3.28$, $c=5.32$ Å for ZnO and $a=4.64$, $c=2.99$ Å for TiO_2 are in good agreement with the observations. By referring hexagonal Zn, Ti metals and O_2 molecule as chemical reservoirs, heat of formation of ZnO and TiO_2 are also calculated, respectively, to be −342.3 and −961.3 kJ/mol, consistent with experimental values of −350.5 and −944.0 kJ/mol.[18] Based on these verified structures, the above surfaces are created. For the inverse spinel Zn_2TiO_4, a structure predicted by DFT and cluster expansion methods is adopted.[19] And surface energy evaluations on three groups of Zn_2TiO_4 {001}, {011}, and {111} suggest that a (010) slab is the most favorable surface terminated by metal-rich and oxygen-rich sides.[16]

A. Adsorption of H_2Se

We first studied atomic Se adsorption on the three surfaces. The adsorption energy is simply evaluated by $E_{ad}=E_{ad}^{tot}-E_{slab}^{ref}-E_{ad}^{free}$, where E_{ad}^{tot} and E_{slab}^{ref} are total energies of slabs with and without adsorption species, respectively. The E_{ad}^{free} is the total energy of free adsorbate. For the ZnO($10\bar{1}0$) surface, we considered all symmetrical sites, including two types of on top of oxygen sites, two on top of Zn sites, and two O-O and Zn-Zn bridge sites, as well as hollow sites. Finally, four adsorption sites are obtained after relaxation as labeled 1, 2, 3, and 4 in Fig. 1(a), among which the atomic Se prefers by at least 0.81 eV than other sites to reside on the site 4 bridging higher layer of Zn and O. Further study on H_2Se molecule adsorption is undoubtedly necessary since H_2Se is the predominant chemical form of Se in the coal gasification product stream over a considerable range of temperatures.[2] On the basis of this atomic site, the most favorable H_2Se adsorption configuration is obtained after a series of calculations of the rotation on the Se-Zn bond and also the tilt operation of H_2Se, which is shown in Fig. 1(b). The adsorption energy of H_2Se on this site evaluated by the above formula is found to be −0.62 eV.

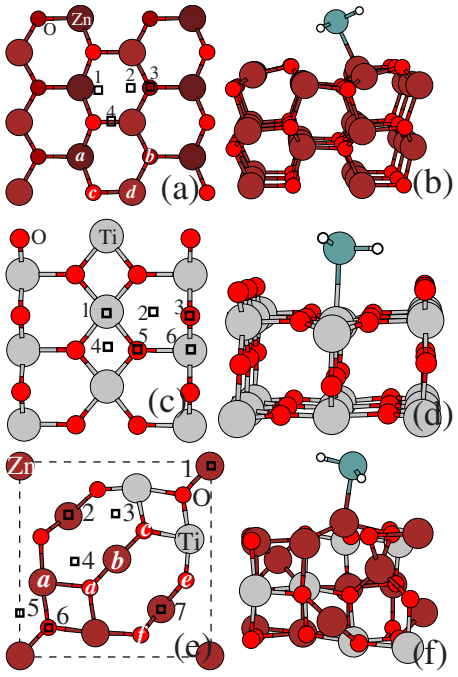

FIG. 1. (Color online) Top view of the adsorption sites (black open squares) of an isolated Se atom on (a) ZnO($10\bar{1}0$), (c) TiO_2(110), and (e) Zn_2TiO_4(010). Side view of the corresponding most favorable configurations of H_2Se on (b) ZnO, (d) TiO_2, and (f) Zn_2TiO_4 surfaces. In (a), the darker balls indicate atoms in lower layers. The white italic letters shown in (a) and (e) are labels for sublimation atoms, which will be discussed in Sec. IV.

Similarly, Se atomic adsorption on rutile TiO_2(110) surface is also studied. The hollow site 2 is found to be the most favorable one among all adsorption sites from site 1 to 6 shown in Fig. 1(c). And Fig. 1(d) displays the most favorable molecular adsorption configuration with adsorption energy −0.27 eV.

Due to the complex nature of Zn_2TiO_4(010) slab, we create this metal-rich surface in a 5×5 mesh, and set a Se atom on each grid point as the initial adsorption configuration. We note that, because of mirror symmetry along diagonal line, the energy difference between the site 2 and 7 is smaller than 0.03 eV. Thus, only several representative final adsorption sites from 1 to 7 are summarized in Fig. 1(e). It was found that a Se atom prefers to bond at site 5 involving a Zn-Zn bridge. Again, based upon this adsorption site, after rotation and tilt of H_2Se calculations, the most favorable molecule adsorption configuration is shown in Fig. 1(f) with adsorption energy −0.66 eV. To verify this favorable configuration, we also calculated adsorption energies of those configurations with H_2Se molecules residing on each of 5×5 grid points of the surface. The above configuration with H_2Se on top of Zn is still the lowest in energy.

To analyze adsorption behavior of H_2Se on different surfaces, we compare Se density of states in adsorbate H_2Se on different surfaces with Se in a free H_2Se molecule. As can be seen from Fig. 2(a), the Se $4p$ states in adsorbate on TiO_2 are broader around −3.8 eV and shifted leftward slightly from −1.0 eV relative to Se $4p$ states in the free H_2Se. While all Se $4s$ and $4p$ states in adsorbate on ZnO and Zn_2TiO_4 are

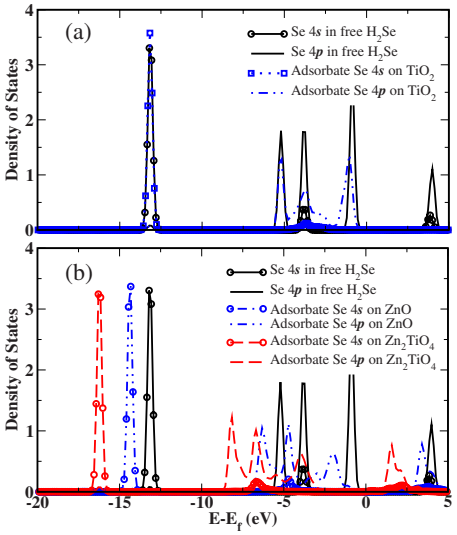

FIG. 2. (Color online) Electronic density of state comparison of Se in free H_2Se with Se in H_2Se adsorbate on (a) $TiO_2(110)$, and (b) $ZnO(10\bar{1}0)$ and $Zn_2TiO_4(010)$.

shifted significantly from those in the free H_2Se as shown in Fig. 2(b). This comparison indicates that relative to adsorbate H_2Se on ZnO and Zn_2TiO_4, the H_2Se on TiO_2 behaves much like free molecule states, implying weaker adsorption energy on $TiO_2(110)$. Further comparison of density of states of substrate atoms where adsorbate residing (cf. Fig. 3) shows that the interaction of Se with substrate Zn atom in ZnO or Zn_2TiO_4 is much stronger than that on TiO_2 because of almost complete overlap of Se $4p$ states with Zn $3d$. This would account for much stronger H_2Se adsorption energy on ZnO, Zn_2TiO_4 than TiO_2, and all can be referred as chemisorption.

B. Dissociation of H_2Se

Having established the preferred adsorption sites for H_2Se on three systems, we now perform systemically studies to

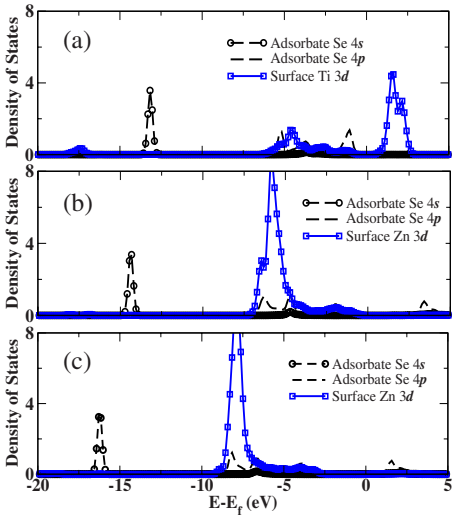

FIG. 3. (Color online) Electronic density of states of Se in H_2Se adsorbate and corresponding surface atom of (a) Ti in $TiO_2(110)$, (b) Zn in $ZnO(10\bar{1}0)$, and (c) Zn in $Zn_2TiO_4(010)$.

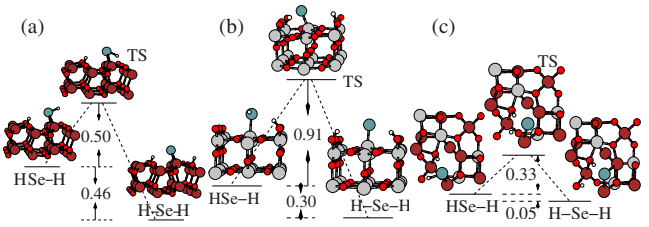

FIG. 4. (Color online) Dissociation pathways from HSe-H to H-Se-H and corresponding barriers on (a) $ZnO(10\bar{1}0)$, (b) $TiO_2(110)$, and a top-view of (c) $Zn_2TiO_4(010)$. The atomic balls are the same as sketched in Fig. 1.

locate the dissociation barriers. Obviously, the whole dissociation process includes a first dehydrogenation ($H_2Se \rightarrow$HSe-H) and a second dehydrogenation (HSe-H $\rightarrow$H-Se-H). By using the NEB method to do this, we need the initial states (H_2Se molecule adsorption) and final states to be specified beforehand. Here, the final states HSe-H refer to HSe segment and H coadsorption. We evaluate the E_{ad} of possible HSe-H coadsorption configurations to find a favorable one. In a similar way, we get the most favorable configurations for H-Se-H as completely dissociated states on the three systems. Notice that even though hydrogen atoms prefer to bond with oxygen, the total energies of two dissociated hydrogen atoms bound with a same oxygen are higher than the most favorable one by at least 0.2 eV on TiO_2, 0.65 eV on ZnO, and 0.99 eV on Zn_2TiO_4. So the two dissociated hydrogen must be binding on different sites. Interestingly, very small barriers ($<$0.08 eV) are found for the first dehydrogenation processes on all three systems. Thus, the H_2Se can be completely dissociated to be HSe-H at typical experimental conditions. For the second dehydrogenation processes, the barriers and associated configurations are sketched in Fig. 4. The HSe-H experience a lowest barrier of 0.33 eV to be H-Se-H on Zn_2TiO_4, an intermediate barrier of 0.50 eV on ZnO and a large barrier of 0.91 eV on TiO_2.

It is easy to understand the different dissociation behavior from coordination number point of view. When a H_2Se molecule adsorbs on the surface, the coordination number of Se changes from 2 to 3. A new bond between adsorbate and substrate depletes electron density between Se and H atoms weakening the bond strength of H-Se-H, and thus the first dissociation barriers on the three systems are all small. For the second dissociation barriers of HSe on ZnO or Zn_2TiO_4, Se atom is hybridizing two surface Zn atoms in a bridge site, which accumulates a relatively large electron density and makes the second H-Se bond weaker. For the second dissociation of HSe on TiO_2, the Se atom remains bonded to only one surface Ti atom, keeping the second H-Se bond strong, thus the dissociation barrier is very high.

C. Kinetic simulations

With the knowledge of the above dissociation barriers, net dissociation rate can be calculated in a standard way by the following Arrhenius expression,[20]

$$r_{\mathrm{dis}} = \frac{k_B T}{h} \frac{\prod_i' \frac{exp(-\hbar\omega_i^{TS}/2k_B T)}{[1-exp(-\hbar\omega_i^{TS}/k_B T)]}}{\prod_i \frac{exp(-\hbar\omega_i^{IS}/2k_B T)}{[1-exp(-\hbar\omega_i^{IS}/k_B T)]}} exp\left(-\frac{\Delta E}{k_B T}\right), \quad (1)$$

where ΔE is the dissociation barrier from DFT calculations, products of numerator and denominator are partition functions of the transition and initial state arising from eigenfrequencies of ω_i^{TS} and ω_i^{IS}. T is temperature and k_B, h are Boltzmann and Planck constants, respectively. The eigenfrequencies of initial and transition states are calculated by the direct frozen phonon method.[21,22] In this method, the elements of the force-constant matrix are calculated from *ab initio* forces, based on which, we can obtain a mass-weighted dynamical matrix which is diagonalized to give the first approximation to the eigenfrequencies and eigenvectors. For each transition state, a single imaginary frequency is obtained.

As indicated above, the H_2Se can be completely dissociated to be HSe-H due to very small barriers. Thus, HSe-H has the same coverage with the H_2Se adsorbate. Then the gross-reaction rates can be yielded by a product of the gas adsorption coverage and the second net dissociation rates. To make a reliable estimation, we considered Langmuir isotherm such that the fractional adsorption coverage can be defined as $\theta = \frac{K_H P}{1+K_H P}$, where K_H is Henry's constant, and P is the partial pressure of gases. To get K_H, we applied a method in the literature[23] $K_H = \frac{K_0 \cdot M_s}{RT\rho_s}$, where M_s is the molecular weight of adsorbate, ρ_s density of adsorbate, and K_0 is ratio of configuration integral of adsorbate to ideal gas phase,

$$K_0 = \frac{Z}{Z_{ig}} = \frac{\int exp[-\beta E(q)] d^{2N+1} q}{\int exp[-\beta E^{ig}(q)] d^{2N+1} q}, \quad (2)$$

where N is the number of atoms in the molecule, $\beta = \frac{1}{k_B T}$, and q is the set of $2N+1$ generalized coordinates describing the position and conformation of the molecules. The integral is performed over the volume of surface adsorbates, in our system, we assumed a height of 2 Å on the unit surface area of supercell. The ideal gas configuration integral Z_{ig} is taken over the same volume as the adsorbates integral Z. The energetics of a dilute adsorbate system can be divided into two contributions: adsorbate intramolecular energy and surface-adsorbate interactions. The adsorbate intramolecular energy describes energy variations arising from conformational changes in the adsorbate molecule alone. For a rigid molecule in our case, H_2Se, the intramolecular energy is zero. Thus, the potential energy arising from surface-adsorbate interactions E is actually the adsorption energy obtained by DFT. For the ideal gas phase, the intramolecular energy E_{ig} tends to zero. The fractional adsorption coverages of H_2Se are then calculated as 3.77×10^{-6}, 3.11×10^{-8}, and 2.79×10^{-5} on ZnO, TiO_2 and Zn_2TiO_4, respectively, and the corresponding gross reaction rates from free molecules to H-Se-H are 1.79×10^4, 0.366 and 1.45×10^6 s^{-1} $site^{-1}$ at 823 K, 1 bar and 2 ppmv conditions. At the relatively low temperature 500 K, the gross rates are 1.46×10^5, 2.52×10^{-3}, and 7.94×10^7 s^{-1} $site^{-1}$ on ZnO, TiO_2 and Zn_2TiO_4, respectively. These estimates indicate that TiO_2 is not active for adsorption of H_2Se while both ZnO and Zn_2TiO_4 should be effective for H_2Se removal but this has not been experimentally tested.

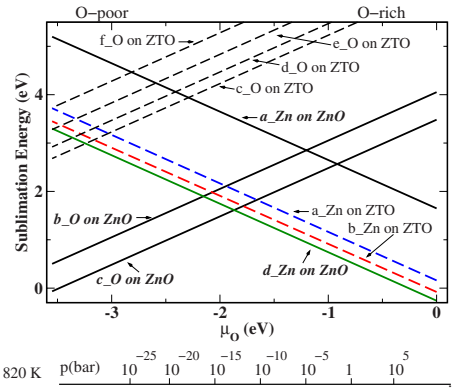

FIG. 5. (Color online) Sublimation energies for the surface atoms on ZnO (solid lines) and Zn_2TiO_4 (dash lines, labeled as ZTO), the atom positions are shown as white italic letters in Figs. 1(a) and 1(e). The label "*d*_Zn on ZnO" means *d* site Zn atom on ZnO surface. Other labels are in a similar way. The μ_O has been correlated with the pressure for a temperature of 820 K.

IV. STABILIZATION EFFECT OF TiO_2

Knowing the H_2Se adsorption and dissociation mechanisms on three systems together with the well-accepted knowledge that ZnO and TiO_2 are two constituent materials of Zn_2TiO_4, a subsequent question is what the role of TiO_2 is. To understand this, it is useful to investigate sublimation energy of surface atoms on ZnO and Zn_2TiO_4. The sublimation energy (E_s) per surface atom is defined as $E_s = E_v^{tot} + \mu_x - E_{slab}^{ref}$, where the total energies of the sublimated-substrate system, the free sublimated atom, and the clean surface are represented by E_v^{tot}, μ_x, and E_{slab}^{ref}, respectively. E_s is the energy that a surface atom gains upon sublimation from substrate to be a free atom. It is defined such that a negative number indicates that the sublimation is exothermic (favorable) with respect to the surface atom and a positive number indicates that it is endothermic (unfavorable). To obtain μ_x, we consider it as $2\mu_O \leq E_{O_2}$; $\mu_{Zn} + \mu_O \leq E_{ZnO}$ for oxygen-rich condition, and $\mu_{Zn} + \mu_O \leq E_{ZnO}$; $\mu_{Zn} \leq E_{Zn}^{bulk}$ for oxygen-poor (Zn-rich) condition.[24] It is also informative to correlate the μ_O to its dependence on the O_2 gas pressure and temperature through the expression $\mu_O(T, p_{O_2}) = \frac{1}{2}E_{O_2} + \tilde{\mu}_O(T, p^0) + \frac{1}{2}k_B T \ln(\frac{p_{O_2}}{p^0})$ as obtained by manipulation of the ideal gas equations.[25,26] Here p_{O_2} is the oxygen pressure and p^0 corresponds to atmospheric pressure. The temperature dependence of $\tilde{\mu}_O(T, p^0)$ in the standard state 1 atm is taken from.[25] With this, for surface atoms on ZnO($10\bar{1}0$), as shown in Fig. 1(a), sublayer Zn, O (labeled as "*a*" and "*b*") and top layer O, Zn (marked as "*c*" and "*d*"), the sublimation energies are evaluated and depicted as solid lines in Fig. 5. Simi-

larly, the E_s of surface atoms on $Zn_2TiO_4(010)$ are plotted as dash lines in Fig. 5. The resulting pressure variation for the range of the μ_O for 820 K is also given. Note that due to mirror diagonal symmetry other nearly degenerate cases are not shown. From comparison with the slope of sublimation energies of surface atoms, it is clear that, under oxygen-rich conditions, all Zn atoms have lower E_s than surface oxygen atoms, where the top layer Zinc [Fig. 1(a) *d*]) on ZnO is smaller than the Zinc atoms *b* and *a* in Fig. 1(e) by 0.18 and 0.42 eV, respectively, indicating that it is relatively easier to form surface Zn vacancies on ZnO than Zn_2TiO_4. On the other hand, this result is also to some extent a reflection of higher thermal stability of Zn_2TiO_4 compared to single metal oxide ZnO.[6] Thus, the additive TiO_2 effectively reduces the formation of surface vacancies on ZnO.

V. CONCLUSION

In summary, from first-principles calculations, we comparatively studied the adsorption and dissociation mechanisms of H_2Se on representative surfaces of $ZnO(10\bar{1}0)$, rutile $TiO_2(110)$ and $Zn_2TiO_4(010)$. We found that H_2Se adsorbs more strongly on the $ZnO(10\bar{1}0)$ and $Zn_2TiO_4(010)$ surfaces than on the $TiO_2(110)$ surface. The dissociation rates on ZnO and Zn_2TiO_4 are found much faster than on TiO_2. The sublimation energies investigations suggest that Zn_2TiO_4 has higher thermal stability than single metal oxide ZnO. The incorporation of TiO_2 offers a stabilization against zinc reduction, which coincides with experiments. Even with the above investigated reaction mechanisms, the problems of the uptake multiple containments (H_2S, H_2Se, and AsH_3, etc.) in coal gasification are more complicated than they might seem at first. On the one hand, we only consider the basic H_2Se dissociation on the pure surfaces and effects from other large volume concentration components, such as H_2 (~35%), CO (~50%), and CO_2 (~10%), are not accounted. On the other hand, in the long run the whole material reaction mechanisms converting to a new bulk material has not yet been established.

*Present address: School of Chemical and Biomolecular Engineering, Georgia Institute of Technology, Atlanta, GA 30332, USA.

[1] J. J. Helble, W. Mojtahedi, J. Lyyränen, J. Jokiniemi, and E. Kauppinen, Fuel **75**, 931 (1996).
[2] M. Díaz-Somoano and M. R. Martínez-Tarazona, Fuel **82**, 137 (2003).
[3] R. A. Newby, E. E. Smeltzer, T. E. Lippert, R. B. Slimane, O. M. Akpolat, K. Pandya, F. S. Lau, J. Abbasiam, B. E. Williams, and D. Leppin, Siemens Westinghouse Power Corporation: Pittsburgh, 2001.
[4] P. Yrjas, K. Lisa, and M. Hupa, Fuel **75**, 89 (1996).
[5] B. K. Gullett and K. Ragnunathan, Energy Fuels **8**, 1068 (1994).
[6] E. Sasaoka, Energy Fuels **8**, 763 (1994).
[7] S. Lew, K. Jothimurugesan, and M. Fkytani-Stephanopoulos, Ind. Eng. Chem. Res. **28**, 535 (1989).
[8] M. Pineda, J. M. Palacios, L. Alonso, E. García, and R. Moliner, Fuel **79**, 885 (2000).
[9] M. Díaz-Somoano, M. A. López-Antón, and M. R. Martínez-Tarazona, Energy Fuels **18**, 1238 (2004).
[10] J. P. Perdew and Y. Wang, Phys. Rev. B **45**, 13244 (1992).
[11] G. Kresse and J. Furthmüller, Comput. Mater. Sci. **6**, 15 (1996).
[12] P. E. Blöchl, Phys. Rev. B **50**, 17953 (1994).
[13] G. Kresse and D. Joubert, Phys. Rev. B **59**, 1758 (1999).
[14] B. Meyer and D. Marx, Phys. Rev. B **67**, 035403 (2003).
[15] U. Diebold, Surf. Sci. Rep. **48**, 53 (2003).
[16] R. B. Rankin, D. S. Sholl, and J. K. Johnson, J. Phys.: Condens. Matter **20**, 095001 (2008).
[17] G. Henkelman, B. P. Uberuaga, and H. Jónsson, J. Chem. Phys. **113**, 9901 (2000).
[18] *Handbook of Chemistry and Physics*, edited by D. R. Lide (Chemical Rubber, Cleveland, 2005), Vol. 86.
[19] R. B. Rankin, A. Campos, H. Tian, R. Siriwardane, A. Roy, J. J. Spivey, D. S. Sholl, J. K. Johnson, J. Am. Ceram. Soc. **91**, 584 (2008).
[20] T. Vegge, Phys. Rev. B **70**, 035412 (2004).
[21] K. Parlinski, Z. Q. Li, and Y. Kawazoe, Phys. Rev. Lett. **78**, 4063 (1997).
[22] G. Kresse, J. Furthmüller, and J. Hafner, Europhys. Lett. **32**, 729 (1995).
[23] E. T. Maginn, A. T. Bell, and D. N. Theodorou, J. Phys. Chem. **99**, 2057 (1995); R. Larry June, A. T. Bell, and D. N. Theodorou, *ibid.* **94**, 1508 (1990).
[24] S. Hao, B. Delley, S. Veprek, and C. Stampfl, Phys. Rev. Lett. **97**, 086102 (2006).
[25] K. Reuter and M. Scheffler, Phys. Rev. B **65**, 035406 (2001).
[26] S. Hao, B. Delley, and C. Stampfl, Phys. Rev. B **74**, 035402 (2006); **74**, 035424 (2006).